International Journal of Computational Vision and Biomechanics
Vol. 5 No. 2 (July-December, 2019)

MUK PUBLICATIONS
Open Access Publisher

Dynamics of the Female Pelvic Floor

Christos E. Constantinou

Stanford University School of Medicine (Urology), Stanford, California, 94395-5118, USA

Submitted: 18th March 2019 *Revised: 13th April 2019* *Accepted: 04th July 2019*

Female urinary incontinence has been recently termed a "silent epidemic", requiring systematic attention and a multidisciplinary approach towards economically ameliorating its impact. In this paper we examine the role of the pelvic floor (PF) in maintaining urinary continence by evaluating the dynamics produced during its voluntary and reflex activation. Analytical methods for the acquisition and subsequent ultrasound analysis of movement of PF structures during maneuvers that are associated with exercises are presented to enable the development of criteria and unique new parameters that define the kinematics of PF function. Principal among these parameters, are displacement, velocity, acceleration and the trajectory of pelvic floor landmarks facilitating functional and anatomical visualization. Different methods of movement detection, including motion tracking algorithms and segmentation algorithms were developed to acquire new dynamic parameters of Pelvic structures during different maneuvers. 2D animation was applied to enhance the ultrasound imaging and highlight the timing of the movement and deformation to fast and stressful maneuvers, which are important for understanding the neuromuscular control mechanisms in urinary continence. Using these visualization technologies changes in linear strain produced as a result of a cough was computed. Parameters were derived from image processing of non-invasive trans-perineal scanning from asymptomatic volunteers as well as patients presenting with relevant pathology. Observations suggest that the timing of response are a significant factors separating the continent from the incontinent subjects in terms of absolute measured parameters as well as computed parameters of linear strain.

Keywords: Ultrasound, biomechanics,

1. INTRODUCTION

Clinical Problem: Functionally the role of the Pelvic Floor (PF) is multiple, ranging from control of urinary and fecal continence to orgasm, conception and birth and in the containment intra abdominal organs such as the uterus, vagina, bladder and rectum. Principal among PF disorders, is urinary incontinence and prolapse, accounting for over 400,000 operations in the USA in 1987 (Delancey 2005), and nearly a third of these were re-operations. It is estimated that 30~50% of women in Europe and the USA are affected by Urinary incontinence (Buchsbaum *et al.* 2005). Stress Urinary Incontinence (SUI), the involuntary leakage of urine on coughing, sneezing, exertion or effort, is the most common form of urinary incontinence in women. The scientific understanding of normal PF function is limited and consequently treatment of these prevalent, disabling conditions is, at best, inefficient. As a consequence SUI has been termed a "hidden epidemic", affects a large percentage of the population, particularly at the later stages of life. In our long-term studies of the mechanism of urinary continence, we realized it is important to develop a method to visualize, measure and model the dynamic responses of the pelvic floor, including the timing of the movement of pelvic structures, consequent trajectories and the dynamic parameters of movement in order to understand the mechanism of urinary continence and establish a more objective basis for the clinical diagnoses and the evaluation of the treatments of SUI patients in clinics.

Anatomical Considerations: Due to the location of the PF defining its normal function is challenging. The PF is under neural control and is a complex 3D arrangement of muscle and connective tissue, attached to the bony pelvis and sacrum. The PFM is a collective name for the levator ani and ischiococcygeus. The levator ani muscle consists of the pubococcygeus, the puborectalis, and the iliococcygeus muscles. The pubococcygeus and the puborectalis muscles form a U-shape as they originate from the pubic bone on either side of the midline and pass behind the rectum to form a sling. The iliococcygeus muscle arises laterally from the arcus tendineus levator ani and forms a horizontal sheet that spans the opening in the posterior region of the pelvis, thereby providing a "shelf" upon which the pelvic organs rest (DeLancey *et al.* 1998). The muscles and fascias of the pelvic diaphragm are inserted on the ischial spines either directly or indirectly through the sacrospinous ligament and the tendinous arch of the pelvic fascia. The result of a PFM contraction can be thought to be a medial pull on the ischial spines to produce a more rigid and narrower PF (Abitbol 1988).

Functional Considerations: Many measurement tools for PFM function quantify the strength of contraction but PFM strengthening is not the only intervention used clinically in rehabilitation of patients with PFM disorders. Indeed there are many methods of measuring PFM activity such as palpation, visual observation, electromyography, dynamometers, ultrasound, and magnetic resonance imaging (MRI). Each tool has its own qualities and limitations (Bo and Sherburn 2005). Most recently, using a reliable instrumented speculum, incontinent women demonstrated lower values in passive force, endurance and speed of contraction than continent women, however, differences

between the two groups for maximal force reached the statistically significant level only in the endurance parameter (Morin, *et al.* 2004). PFM strengthening exercises do diminish the symptoms of SUI (Berghmans, Hendriks et al. 1998; Norton, Chelvanayagam *et al.* 2003) yet a number of studies have demonstrated that strength of PFM contraction does not always correlate to continence state or action on the urethra (Kessler and Constantinou 1986; Theofrastous *et al.* 2002; Morin, Bourbonnais *et al.* 2004), so what is it about PFM rehabilitation that helps? Little research has focused upon the mechanisms of therapeutic change to help identify the specific critical muscle components of training (Nygaard 2004) so it is unknown whether PFM training mimics the normal physiological behavior of the PFM or is an compensation strategy, nor whether a strengthening program is indeed the most efficient method of conservative rehabilitation. It seems appropriate to determine whether other properties of muscle function are also important in defining PFM function and dysfunction, as well as gaining a greater understanding of why PFM rehabilitation in women with SUI is effective.

Contribution of Imaging: Previous visualization studies using ultrasound or MRI show that a voluntary contraction of the Pelvic Floor Muscles (PFM) changes the ano-rectal angle (ARA) (Costantini *et al.* 2006) and can displace the urethra in a direction towards the pubic symphysis (Miller *et al.* 1998, Miller, *et al.* 2001; Constantinou *et al.* 2002; Dietz *et al.* 2002, Dietz 2004). Yet why does a correct PFM contraction in some women increase the intra urethral pressure, but in others it does not? (Bump *et al.* 1991) It is known that in continent women there is recruitment of PFM motor units (Deindl *et al.* 1993) and an increase in intra-urethral pressure (Constantinou and Govan 1982) prior to an increase in intra-abdominal pressure (IAP) during a cough. Is the increase in intra-urethral pressure caused by an automatic, pre programmed activation of the PFM? If so, is this pre-activation lost or delayed in SUI? Certainly there are altered PFM activation patterns during a cough, measured by EMG in women with SUI compared to healthy volunteers (Deindl *et al.* 1994), with shorter activation periods, lack of response or paradoxical inhibition, so how does this alteration affect the trajectory of urogenital structures?

Visualization studies have described the displacement of the urethra or bladder neck that occurs from the start to finishing point of a cough, a PFM contraction and Valsalva maneuver, yet none so far have either mapped the trajectory throughout the maneuver, or defined the automatic function of the PFM, especially in response to sudden rises in intra-abdominal pressure (IAP) during a cough. Are the differences in women with PF disorders just a difference of amplitude of displacement, or are the specifics of the journey important too?

The PFM, along with the diaphragm and abdominal muscles are also thought to contribute in generating intra-abdominal pressure (IAP). Disorders of breathing and incontinence have a strong association with low back pain (LBP) (Smith, Russell et al. 2006) and subjects with LBP generate more IAP during low load tasks and have alterations in the timing of trunk muscle activity (Hodges and Richardson 1999; Ferreira, Ferreira et al. 2004) than those without LBP. Small studies of continent women have shown that the Abdominal muscles and PFM co-activate(Sapsford et al. 2001; Neumann and Gill 2002), is this true for a larger group size, and are there any differences in women with SUI or other PF disorders? To answer those important clinical questions, it is essential to establish reliable methods for the evaluation of the PF function. The reliable methods to evaluate the changes of the PF functions will be helpful for the physicians or clinicians to identify those patients who are likely to be rehabilitated by PF exercises instead of by surgery.

MRI imaging was introduced to study the anatomical components of the PF and thereby contribute to better understand mechanism of continence (Klutke, Golomb *et al.* 1990; Yang, Mostwin *et al.* 1991; Christensen *et al.* 1995; Stoker *et al.* 2001). Different methods have been applied to process and analyze the MRI image to acquire the 2D anatomy of the PF with higher spatial resolution and speed of image acquisition (Comiter *et al.* 1999; Goh *et al.* 2000; Gousse *et al.* 2000). MRI imaging in 3D, reported in the recent research literature, was achieved by reconstructing sequential 2D images acquired in the axial and sagittal plane (Athanasiou *et al.* 1999; Fielding, Dumanli *et al.* 2000). While 3D MRI imaging provides very useful insight into the anatomical configuration, the amount of time required to acquire 3D volume data is too long to record any dynamic information of the PF activities. Therefore, current 3D MRI studies are limited to analyze the passive response of the PF under a certain loading or straining (Stoker *et al.* 2001). MRI imaging is also too expensive to be used in regular clinical examination.

Diagnostic Methods. In current clinical practice, manual muscle testing per vagina is the technique used by most clinicians to evaluate a PFM contraction using a 5 point modified Oxford Grading ordinal scale (Laycock and Jerwood 2001). It can measure whether or not there is a correct contraction and the strength of it. The main limitation of this method is the length of time the assessment takes and the ease with which most clinicians, other than physiotherapists, could incorporate it into their clinical practice. Vaginal palpation has also been criticized for its lack of reliability and sensitivity in the measurement of pelvic floor muscles strength for scientific purposes (Bo, Lilleas *et al.* 2001). Because of the inherent limitations of vaginal palpation, other methods such as vaginal cones, hydrostatic pressure, surface, needle and wire EMG are currently tested to assess PF function and the improvement of PF function in conservative treatment. The clinical applications of those methods are limited because they are invasive and inconvenient to be applied in regular clinical examination.

2D ultrasound imaging can acquire dynamic information on the morphology of the urogenital organs. In particular, perineal, introital and trans-vaginal ultrasound has become an imaging platform for the evaluation of the PF and for the treatment planning of many uro-gynecological conditions (Bo *et al*. 2001). By its nature, 2D ultrasound imaging provides a very large amount of dynamic data that cannot be visually assimilated by the observer in its totality, particularly during fast occurring events. Such dynamic events contain information relating the integrity of the supporting structures of the bladder neck, the role of the PF, and the compliance of pelvic floor structures (Barbic, Kralj *et al*. 2003). Furthermore, because the urogenital structures are anatomically interconnected, ultrasound-based dynamic imaging can substantiate urodynamic observations of the effective distribution of pressure transmission to the urethra. State-of-the-art 3D ultrasound imaging techniques provide 3D visualization of the pelvic floor structures with higher resolution. However, current 3D ultrasound machines are not fast enough for the purpose of visualization the movement of tissues in fast and stressful maneuvers like coughing, which may provoke urinary incontinence. Besides, as 3D imaging is cost prohibitive for the majority of clinicians it is anticipated that 2D ultrasound will be, for the foreseeable future, the measuring and feedback tool of clinical choice.

Evaluation of the dynamic function of the PF using 2D ultrasound imaging. In real time ultrasound imaging, the diagnostically important information of the dynamic response of the PF cannot be assimilated and quantified by the observer during the scanning process. The trajectories and the timings of the movement of the PF tissues, which may be more important than the amplitudes in the mechanism of female urinary continence, are usually ignored. Current quantitative measurements of 2D ultrasound images can only tell us about the resting position of the urethra and the displacement at the end of events such as Valsalva, voluntary PFM contraction and coughing. The difficulties with accurately determining the finishing point of any maneuver, are numerous and are a potential source of error. The operator has either had to make multiple on-screen measurements, or determine the exact peak moment, or end position of the maneuver, freeze it, and then measure the change in position manually on screen or within in built electronic calipers. Without correcting for probe movement relative to the pubis symphysis the percentage errors range from 18-87%. In addition measuring only the re-positioning of urogenital structures is of limited value because intermediary anatomical changes are not registered.

In order to develop more sensitive measures to define normal PF function pilot studies were performed to capture and visualize the sequence of dynamic changes the PFM produced on the urethra, vagina and rectum using digital image-processing methods. The approach taken is to use an edge extraction algorithm to outline the coordinates of the symphysis, urethra and rectum interfaces on a frame-by-frame basis for sequences of stress inducing events such a cough, Valsalva and voluntarily induced PF contractions. During each event, the trajectory of the boundary of each structure was identified to characterize the sequential history of the ensuing movement. The resulting image analysis focused to reveal the anatomical displacement of the urogenital structures and to enable the evaluation of their biomechanical parameters in terms of displacement, velocity and acceleration. On the basis of these observations, we expect that the urogenital response to PF contractions can be quantified and the mechanism of UI, including the trajectories and timing of the PF activities, can be elucidated. Given that ultrasound imaging contains a considerable amount of useful data which can be obtained with the minimum of invasion to the patient, it is appropriate to find a way that this information be revealed, displayed quantitatively and quantitatively measure, analyze and describe the whole of the movement during a particular maneuver. We have accounted for movement of the probe, relative to the structures being examined and do not rely upon the operator to capture the precise moment at the end of the maneuver. Confidence is required none the less to validate the ultrasound approach with subjects of a broad age group and disposition. The visualization of the PF activities using 2D ultrasound imaging is likely to develop new measures of the PF functions that are more sensitive and specific than current methods. Those measures are useful for categorizing different sub groups of patients within a particular pathology and determining the most appropriate treatment intervention.

2. METHODS

2.1 Coordinate System of the Anatomic Structures

Visual examination of the ultrasound images suggested that the displacement of the PF tissues during maneuvers contains components that can best be defined as a ventral (anterior) component towards or dorsal (posterior) component away from the symphysis pubis and a cephalad (superior) component upwards or caudad (inferior) component downwards. This is supported by other studies that suggest that in a functional PFM contraction, the bladder neck has been shown to move in a ventro-cephlad direction increasing the closure pressure within the urethra as it is displaced towards the symphysis pubis and during valsalva, as the intra-abdominal pressure (IAP) increases, the bladder neck moves in a dorsal-caudad direction.

Therefore, an orthogonal coordinate system fixed on the bony landmark, the symphysis pubis, was established (Figure 1). The two axes of the coordinate system are parallel and vertical to the urethra at rest respectively. The coordinate system is fixed during the maneuver, so when the subject deforms the bladder (State 2 in Figure 1), the coordinate system will maintain its original position and the ensuing trajectory of urogenic structures can be measured relative to this fixed axis.

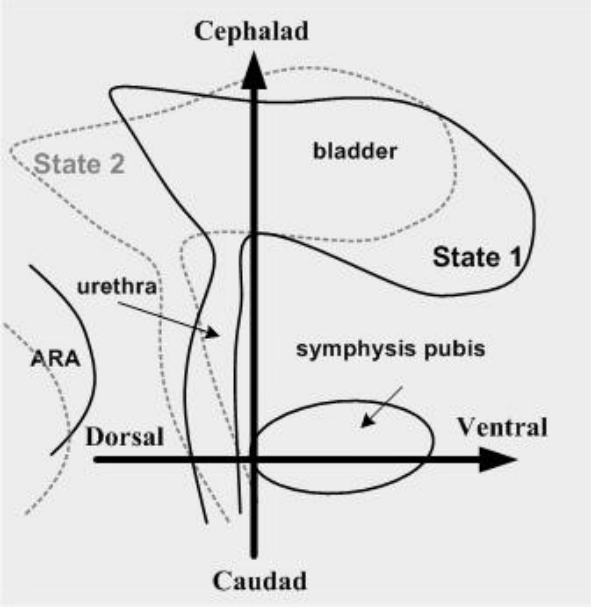

Figure 1: The orthogonal coordinate system fixed on the symphysis pubis. The two orthogonal components (ventral-dorsal and cephalad-caudad components) of the tissues displacements reflect PF functions of squeezing the urethra and supporting the bladder respectively. (Reprinted from Peng *et al.* 2007)

2.2 Motion Tracking Algorithms

A readily visible, clearly resolved anatomical structure in perineal ultrasound imaging is the angle the rectal ampulla forms with the anal canal, the ano-rectal angle (ARA). The movement of ARA can be used to analyze the PFM function because the sling of the PFM or Levator Ani muscles wrap around the anorectal junction, and its displacement is closely associated with a PFM contraction

In order to accurately map the trajectory of the ARA in response to a cough it is necessary to maintain each frame indexed to the symphysis pubis, which is a stationary, rigid, non deforming structure. However, the movement of the ultrasound probe in experiments could cause a motion artifact in the image of the symphysis pubis. Therefore, the motion artifact of the symphysis pubis needs to be tracked and subtracted from the motion of the ARA. To accomplish the task of indexing, we developed an adaptive motion tracking algorithm based on matching template to measure the movement of the symphysis pubis.

Initially, a template of the symphysis pubis is manually defined in the first frame of the ultrasound video. The template is then compared with the second image frame with different offsets in both x and y direction. The matched position in the second image frame is defined as the position where the difference function $D(k, l)$, given by Equation (1), has the minimum value.

$$D(k,l) = \sum_{i=0}^{M-1}\sum_{j=0}^{N-1}\left|T_{i,j} - P_{i+k,j+l}\right| \quad (1)$$

where, $T_{i,j}$ and $P_{i+k,j+l}$ are the template and the image to be matched respectively. M and N is the size of the template. k and l are offsets for matching at different position.

The template for the matching the following image frames is then updated according to Equation 2 and the matching procedure is repeated until the last image frame.

$$T(n) = \frac{1}{n}\sum_{i=0}^{n-1} S(i) = \frac{n-1}{n}T(n-1) + \frac{1}{n}S(n-1) \quad n \geq 2 \quad (2)$$

where, $S(i)$ is the matched position of the symphysis pubis in image frame i.

A similar adaptive matching algorithm is used to track the motion of ARA. However, ARA is a soft tissue structure which deforms, particularly in fast maneuvers like coughing. Therefore, a weight coefficient is introduced to speed up the updating of the template in order to follow the deformations:

$$T(n) = w \cdot T(n-1) + (1-w) \cdot S(n-1) \quad n \geq 2 \quad (3)$$

where, w is the weight coefficient, $w \in [0, 1]$. In practice, w is set to a value between 0.7 and 0.8 according to the extent of the ARA deformation.

To decrease the effect of the size and position of the initial template, manually defined in the first image frame, the tracking procedure is performed four times with different initial templates and the results are averaged. The relative movement of ARA to the symphysis pubis is then derived by subtracting the motion of symphysis pubis from that of ARA.

Figure 2 illustrates the results of the motion tracking of a healthy subject's symphysis pubis and ARA in supine. Figure 2 (a) shows the ultrasound image at rest and the ventral-cephalad coordinate system. The motion tacking of the symphysis pubis and ARA are shown in Figure 2 (b) and (c) respectively. The relative movement of ARA shown in Figure 2 (d), is derived by subtracting the motion of symphysis pubis from that of ARA and then transforming the image coordinate system to the ventral-cephalad coordinate system.

2.3 Image Segmentation Algorithms

Because the urogenital structures are anatomically interconnected, ultrasound based dynamic imaging can substantiate urodynamic observations of the effective distribution of pressure transmission to the urethra closure mechanism. However, urethra and bladder, which are the container or path of the urine, may have huge deformation in maneuvers. The above-mentioned motion tracking algorithms based on matching are not applicable in the movement analysis of the urethra and bladder.

Therefore, an image segmentation algorithm needs to be designed to segment the boundaries of the urethra and bladder. The movement analysis of the urethra and bladder can then be based on the tracking of the typical anatomic position, such as Urethro-Vesical Junction (UVJ), on the boundaries of the urethra and bladder.

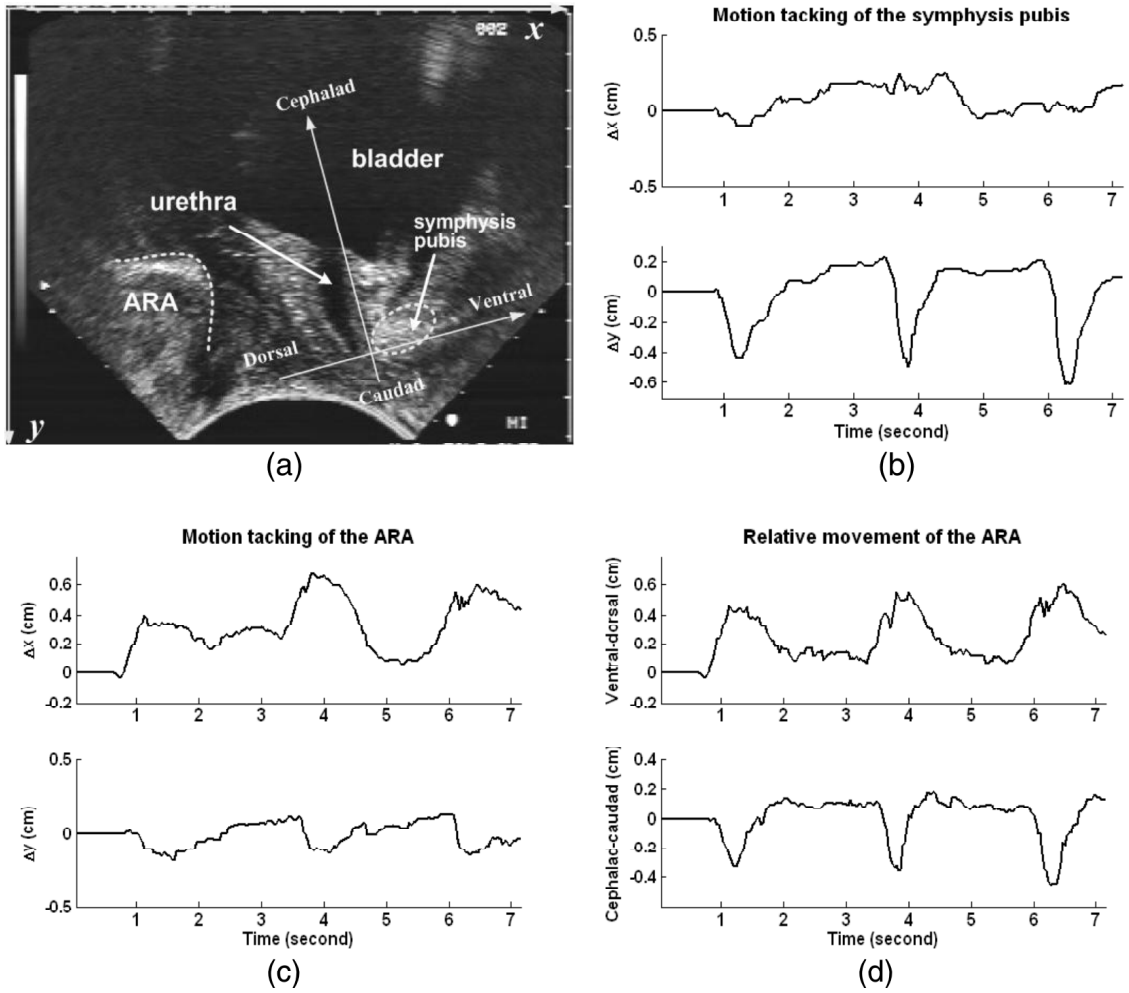

Figure 2: The motion tracking of a healthy subject's symphysis pubis and ARA in supine. (a) The ultrasound image and the coordinate system. (b) The motion tracking of the symphysis pubis and the ARA (c). (d) The ventral-dorsal and cephalad-caudad components of the displacement of the ARA. (Reprinted from Peng *et al.* 2006)

Test results show that the segmentation algorithms usually do not work well because of the speckle noise in the ultrasound images, the movement and out-of-plane rotation of the ultrasound probe, and especially the huge deformations of the urethra and bladder during fast, stressful maneuvers like coughing. Therefore, a simple and effective segmentation algorithm based on "virtual ruler" was developed for the segmentation of the urethra and bladder.

To begin, the original ultrasound images with integer values were converted to binary images with logical value of 0s (black) and 1s (white). Otsu's method, which minimizes the intra-class variance of the black and white pixels, was used to determine the threshold for the conversion. All pixels in the intensity image with value less than the threshold have value 0 (black) in the binary image. And all other pixels have value 1 (white) in the binary image. Then, the isolated pixels (individual 1's that are surrounded by 0's) were removed from the binary images by combining morphological operations of dilation and erosion.

The boundaries of interior and posterior edges of urethra and bladder were then segmented in the binary images using the automatic segmentation algorithm shown in Figure 3. An initial point on the edge to be segmented was chosen, and one end of a virtual ruler was fixed on the initial point. The virtual ruler was then rotated around the initial point until it hit a non-zero point on the edge. The fixed end of the virtual ruler was then moved to the non-zero point. The virtual ruler was rotated around the fixed point again until it hit a new non-zero point on the edge. The procedure of moving and rotating the virtual ruler was repeated until the contour of the whole boundary was acquired. The length of the virtual ruler is an adjustable parameter to obtain different resolution of the segmentation. The shorter the virtual ruler, the more detailed information will be elucidated in the segmentation. However, the results of the segmentation will be affected by the noise in the ultrasound images if the virtual ruler is too short. Therefore, the length of the virtual ruler was set from 4 pixels to 16 pixels. After the segmentation, smoothing spline, a nonparametric fitting method available in MATLAB® curve-fitting toolbox, was applied to smooth the segmented boundaries of tissues. The smoothing parameter was set to p=0.8 to obtain the most reasonable results.

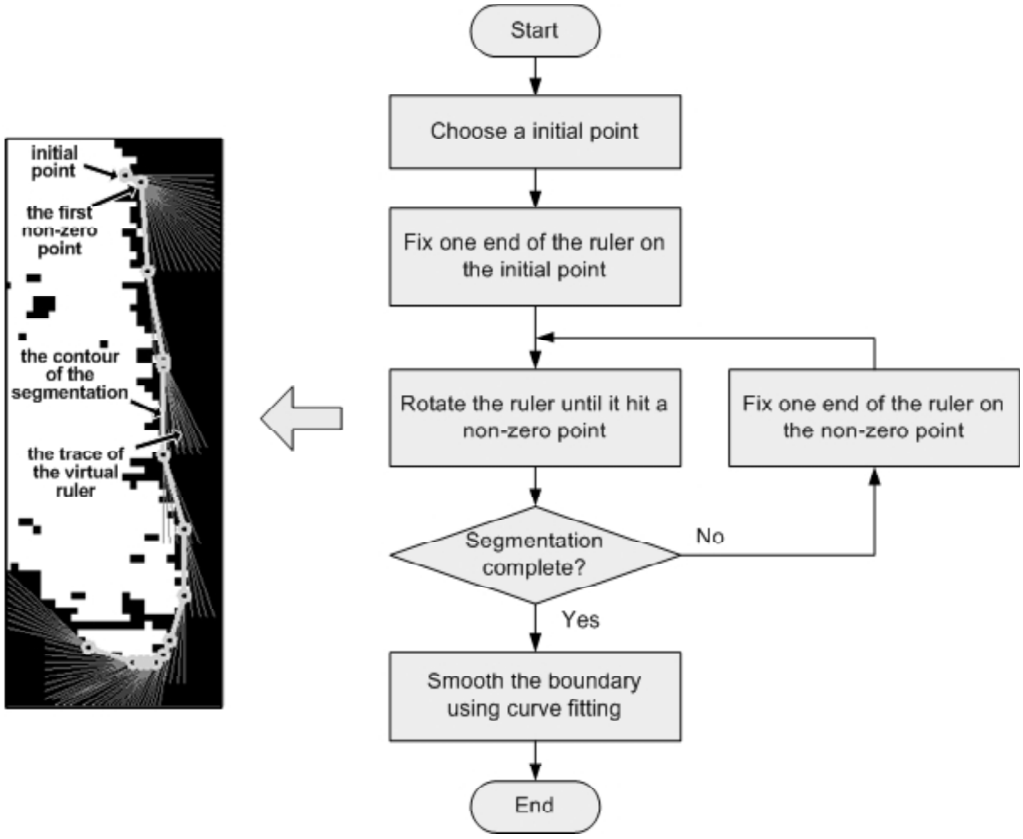

Figure 3: Flow chart of automatic image segmentation. (Reprinted from Peng *et al.* 2006)

After the images were segmented an orthogonal system with its origin fixed on the symphysis was established assuming an ellipsoidal pubis. The two axes of the coordinate system are parallel and vertical to urethra points P_1 and P_2 are illustrated by Figure 4 at the resting position. Based on the ultrasound images it has been suggested that the displacement of the ARA during the maneuvers can be described as ventral component toward the SP or as a forward component and a lift component.

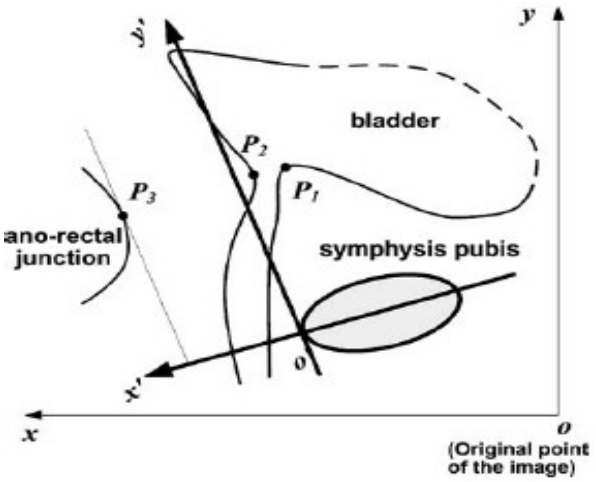

Figure 4: The coordinate system fixed on symphysis pubis (x'-o'-y') in the ultrasound images during motion tracking (Reprinted from Peng *et al.* 2006)

After the coordinate system has been established, the trajectories of the boundaries of the ARA were overlaid to characterize its sequential movement. A point P on the ARJ was chosen to describe the trajectory of its movement and the displacements in the ventral-dorsal and cranial-caudal direction of that point were measured during all the maneuvers. The ultrasound images of the motion tracking of the ARA junction is shown in Figure 5 during the cough, PFM contraction and Valsalva.

2.4 Strain Measurements

Based on the reported results by Peng *et al.* 2007, Figure 6 illustrates the displacement history of the Cough maneuver wa to evaluated the response of the system using the tracking of ARA. Thus using the numerical values of these displacement measurements, strain can be calculated .by drawing a straight line from the symphysis pubis to the midpoint of the ARA.

The strain at time *t* is defined as: $\varepsilon_t = \frac{\| \vec{L}_t \| - \| \vec{L}_0 \|}{\| \vec{L}_0 \|}$ (1)

where $\| \vec{L}_0 \|$ (represented as a green vector in Figure 5) is the initial length of the pelvic floor muscle at rest and is measured from the ultrasound images.

$\| \vec{L}_t \|$ is the length of the muscle at time *t* and is calculated from the equation $\left[\| \vec{L}_t \| = \sqrt{\left(\vec{l}_{t,x}\right)^2 + \left(\vec{l}_{t,y}\right)^2} \right]$ .....(2)

Figure 5: Ultrasound images of the motion tracking of the ARA: Outlines of the contours of the urethra, bladder and ARA during (a) cough showing the temporal sequence over a 1.2 second period in three individual frames. (Reproduced from Peng *et al.* 2006).

$\vec{l}_{t,x}$ is the vector representing dorsal-ventral component of the pelvic floor muscle at time *t* and is measured by the equation $\vec{l}_{t,x} = \Delta\vec{x} + \vec{l}_{0,x}$ ……. (3), and likewise $\vec{l}_{t,y}$ is the vector representing cardinal-caudal component of the pelvic floor muscle at time *t* and is defined by the equation $\vec{l}_{t,y} = \Delta\vec{y} + \vec{l}_{0,y}$ …….(4).

Where $\vec{l}_{0,x}$ and $\vec{l}_{0,y}$ (dashed blue vectors in Figure 5 (e)) are the dorsal-ventral and cardinal-caudal vector components of the pelvic floor muscle at rest (t = 0) respectively. $\Delta\vec{x}_t$ and $\Delta\vec{y}_t$ are the dorsal-ventral and cardinal-caudal displacements, respectively at time *t* , which can be measured from the previous displacement measurements from the Peng *et al* paper as shown in Figure 5 (in this figure $\vec{A}_t$ (in blue) represents the vector $< \Delta\vec{x}_t, \Delta\vec{y}_t >$).

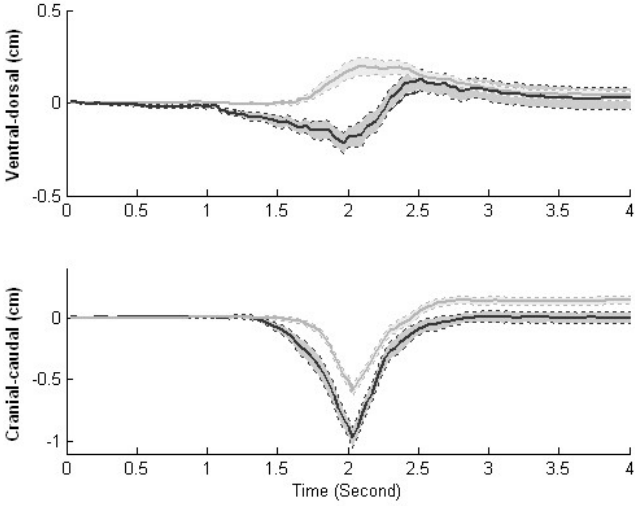

Figure 6: Dorsal-ventral and cardinal-caudal movement of ARA during the cough maneuvers: The continent subjects and the SUI patients are shown in green and red respectively. The SE of the movement is marked by the colored areas with the dotted lines as the boundaries of SE (Peng *et al.* 2007).

In order to carry out the vector addition in Equation 2, it was necessary to retrieve the $\Delta\vec{x}_t$ and $\Delta\vec{y}_t$ values from the graphs shown in Figure 6. The mean of those values was calculated, and an array was made for the average time measurements. Then the displacement measurements in the dorsal-ventral and cardinal-caudal directions corresponding to those average time values were added and the array was entered into a new Microsoft Excel spread sheet. Using the Microsoft Excel formula feature, the $\vec{l}_{0,x}$ and $\vec{l}_{0,y}$ vectors, measured from the ultrasound images shown in Figure 7, were added to the corresponding displacement measurements according to **Equations 3** and **4**. The strain was also calculated according to **Equation 2** at each of the time values. Then using the excel graphing feature, the strain vs. time graph was graphed for each of the four maneuvers in the supine position and also in standing position for the cough in both healthy and SUI patients. Subsequently the maximum strain of the PFM for both groups was obtained and compared between the two.

2.5 Strain Rate Measurements

As previously reported, the velocity of ARA during cough from the time derivative of displacement for both groups evaluated was calculated and is shown by Figure 8.

Using these velocity measurements along with the displacement measurements, the strain rate of PFM for healthy and incontinent women during a cough was calculated.

Strain rate (SR) can be measured using the following equation:

$$\frac{dL}{L} \approx \frac{v\ (r+\Delta r) - v(r)}{\Delta r} dt = SR\ dt \quad \text{...(5) (Gilja } et\ al. \text{ 2002).}$$

Where here *r* represents the position of the point on the ARA, thus $\Delta r = \| \vec{L}_t \|$, which is defined by (2).

Also $v\ (r+\Delta r) - v(r) = \Delta v = \sqrt{(\Delta v_x)^2 + (\Delta v_y)^2}$ …… (6).

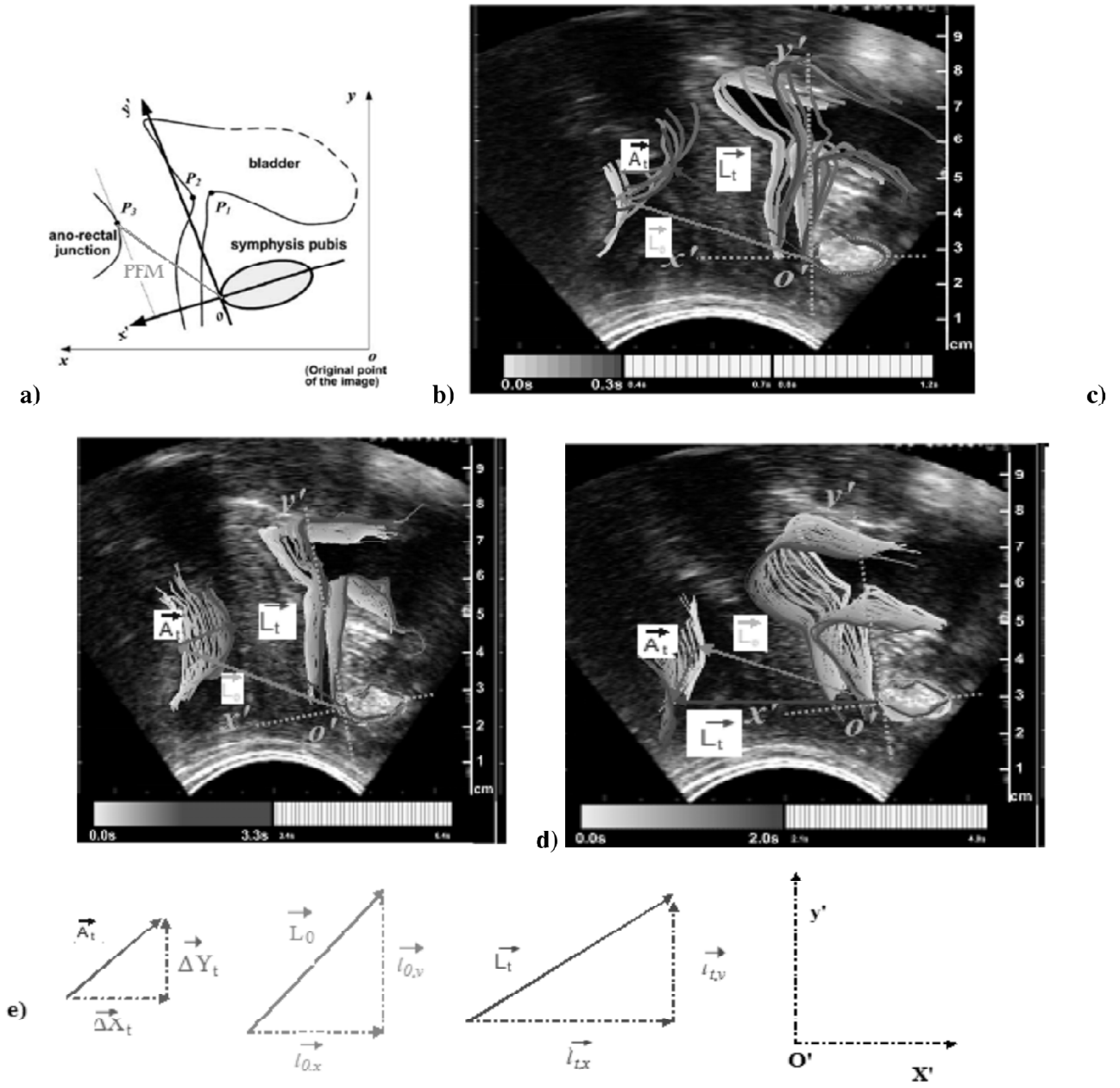

Figure 7: Vector Representation of the PFM. PFM is simplified as a straight line from SP to ARA (a); Vectors $\vec{L}_t$ (purple vector representing length of the PFM at time t), $\vec{L}_0$ (green vector representing length of the PFM at rest), and $\vec{A}_t$ (blue vector representing the resultant vector of the displacement vectors $\Delta\vec{x}_t, \Delta\vec{y}_t$ at time t) are shown in ultrasound images of a SUI volunteer during a cough (b), voluntary PFM contraction (c) and valsalva (d); the dorsal-ventral (x') and cardinal-caudal (y') components of the vectors $\vec{A}_t, \vec{L}_0$ and $\vec{L}_t$ are represented and the fixed coordinate system (black dashed lines) is displayed on the right (e).

Strain rate is related to strain by the equation $\varepsilon = \exp(\int_{t_0}^{t} SR \ \ dt) - 1$ …(7), and that is because strain rate is defined as the time derivative of natural strain ($\ln \frac{L}{L_0}$) (Gilja *et al*. 2002).

From **Equation 5,** the strain rate was calculated and the strain rate vs. time was graphed for the two groups and the maximum strain rate was calculated and statistically compared for significant differences using a standard T-test.

3. RESULTS

3.1 Strain During Cough

Figure 9 illustrates the comparative differences between continent and SUI women measured during a cough in standing position. This figure suggest that in a standing

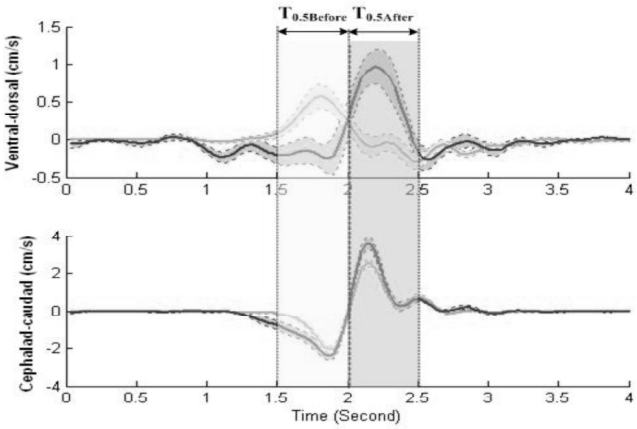

Figure 8: Ventral-dorsal and cranio-caudal components of the velocity of the ARA in supine during a cough. The controls(green) SUI (red). The SEs of the signals are marked by the colored areas (Reproduced from Peng *et al.* 2007).

position the strain of the PFM in SUI women does not reach a maximum negative strain as in healthy individuals, rather it increases in the positive direction. Furthermore, Figure 9 illustrates that for healthy individuals the amplitude of maximum negative strain in standing position is much less than of the strain during a cough than that in the supine position. And as for the SUI women, the strain vs. time pattern during a cough in the standing position is completely different from that of supine position since the strain in the standing position increases in a positive direction as opposed to a negative direction seen in a supine position.

The statistical summary given by Table 1 shows the maximum strain of PFM during a cough in supine and standing position for the SUI and healthy individuals along with the significance of difference between the standing and supine position and also between the two groups. It can be denoted from Table 1 that there is a significant decrease (p value of < 0.001) of the maximum strain in healthy

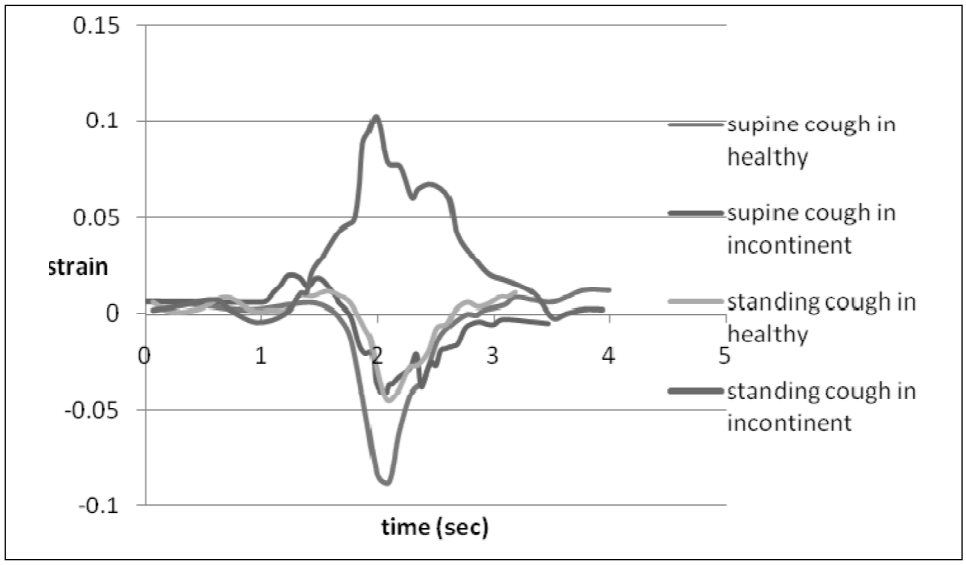

b)

Figure 9: Strain of the PFM over time comparing healthy and SUI subjects during a cough in standing position and supine position.

individuals from supine to standing position. That is the maximum negative strain is 48.8% ± 7.3 % higher in the supine position than that in the standing position. As for the SUI patients, the maximum strain values for the standing position and supine position significantly differ (p value of < 0.0001) by 343.9% ± 85.3 %. The PFM strain in standing position during a cough is also significantly different between SUI and healthy patients (p value of < 0.0001) with percentage difference of 322.2% ± 97.0 %.

3.2 Strain Rate

Figure 10 illustrates the differences between continent and SUI women for the strain rate of PFM during a cough in supine position. While both groups have similar patterns in the strain rate the SUI women have a much larger maximum positive and negative strain rate than the healthy individuals.

Table 1
Maximum strain of the PFM in healthy and SUI women during a cough in supine and in standing position with p values showing the degree of difference between the two position and the two groups

	ε max (Controls)	*εmax (SUI)*	*P (Controls/SUI)*
Cough, supine	-0.088 ± 0.007	-0.041 ± 0.002	< 0.0001
Cough, standing	-0.045 ± 0.003	0.10 ± 0.04	< 0.0001
P (Supine/ standing)	< 0.001	< 0.0001	

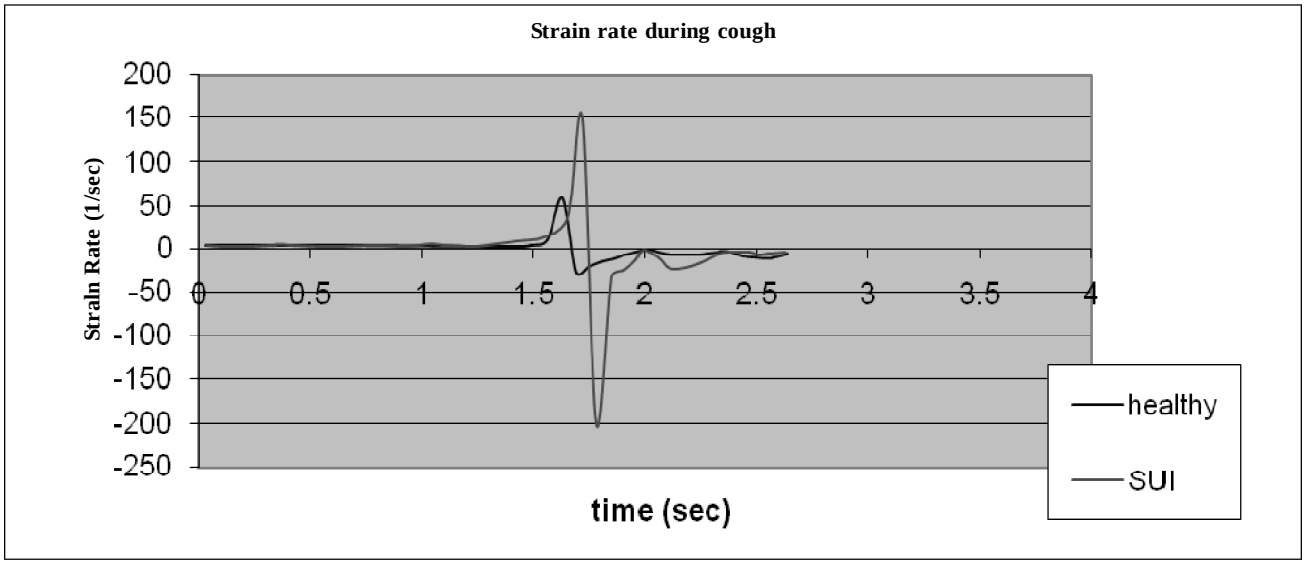

Figure 10: Strain rate of the PFM over time in healthy (blue graph) and SUI (pink graph) patients during a cough in supine position

The statistical summary given by Table 2 shows the mean and standard error measurements of the maximum negative strain rate of the PFM during a cough in supine position for the SUI and healthy individuals along with level of significance. As indicated the maximum strain rate in SUI patients is significantly higher than that of continent individuals with SUI patients having a strain rate that is 716.4% 73.3% higher than the healthy subjects (p value <0.0001).

Table 2
Maximum negative strain rate of the PFM in healthy and SUI women during a cough in supine position with p values showing the significance of difference between the two groups

Cough (Supine)	*Strain Rate (strain/sec)*	*P value*
Controls	-27.4 ± 0.5	< 0.0001
SUI	-199.2 ± 0.7	< 0.0001

4. DISCUSSION

In this publication we have extended the analysis of existing results of ultrasound imaging in an efford to obtain quantification of new dynamic biomechnical parameters of PFM function. Our approach of processed ultrasound imaging of the pelvic floor provides significant new information relating to its dynamic response to stress. We generated this non-invasive type of new information in order to understand the mechanisms of urinary continence, which is a silent epidemic severely affecting the quality of life of women with Urinary Incontinence. Potentially, this approach can help lay the foundations of determining a more reliable pragmatic assessment of PFM function and eventually improve the rehabilitation of women with SUI and other pelvic floor disorders. Furthermore these studies suggest that the anatomical and physiological changes of the PF in women with SUI can be highlighted by analyzing the activities of critical anatomical structures, their biomechanics and response to the cough reflex. In this way, through 2-D ultrasound image processing we extended the analysis and visualization of the static and dynamic responses of these structures to hopefully provide a sensitive and reliable tool for better clinical diagnoses. More specifically, in this paper the linear strain of the PFM muscle in the mid-sagital plane was calculated during for the cough, maneuver using previous kinematic measurements obtained from motion tracking using 2-D ultrasound imaging techniques Jones *et al.* 2006 a,b. Our analysis has shown that during the cough, there was a highly significant difference between the maximum strain of the PFM in SUI women and healthy women in both standing and supine position. This 53.4 ± 5.5% difference further supports the observation that the strain as a parameter plays an active role in determining continence. One recent mechanism suggests that pelvic floor muscles contract in reaction to increases in intra-abdominal pressure, which a cough causes such pressure. This contractions cause the pelvic organs to lift and the vaginal canal to compress and thus compressing the urethra which helps to prevent leakage (Mclean *et al.* 2007). In the standing position, during a cough, the maximum strain of the PFM was -4.5% ± 0.3% for healthy individuals. This 48.8% ± 7.3% difference supports the theory that while standing the PFM has already been activated, and thus since the muscle is already loaded, it would contract less than that in a lying position (Petros *et al.*, Shishido *et al.* 2006). This phenomenon have been attributed to the idea that change in posture causes the vaginal closure force to increase due to higher IAP and greater resistance of the PFM. As for the SUI patients the maximum strain of the PFM in a standing position during a cough was 10.0% ± 4.0%, which is a positive value differing by 343.9% ± 85.3% from that of

supine position. This result suggests that the PFM in SUI patients do not go through a further contraction in standing position, rather it stretches. This can imply that the PFM in SUI patients loses its ability to contract in a loaded position and undergoes passive deformation from external forces.

In this paper, the maximum negative strain rate of the PFM during a cough in supine position was also measured for the two groups. This value was -27.4 ± 0.5 per second for healthy individuals and -199.2 ± 0.7 per second for the SUI women. This is a very notable difference suggesting that although SUI patients have a much lower PFM strain during the cough, the rate of this strain is much higher (716.4 ± 73.3%) than that of healthy individuals which could provide insight into the mechanism of contraction during a fast and abdominal stress causing event. As we have previously discussed the strain of the PFM in SUI can be increasing with such great speed because the PFM loses its ability to slow down the movement of the urogenic structures during a cough in SUI women Jones *et al.* 2007b.

The strain values measured in this paper can be compared to previous strain measurements of the PFM and different muscle tissues. Dietz *et al.* had used 3D translabial pelvic floor ultrasound to measure the strain of pubovisceral muscle fiber during PFM contraction and Valsalva from hiatal circumference measurement of 98 patients. Strain during contraction was calculated to be -15.9 ± 8.4% and 22.7 ± 21.3% during Valsalva (Dietz *et al.* 2006). The direction of these strain measurements is perpendicular to the mid-sagital plane direction used in this paper. The strain value of -2.9 ± 0.9% measured in this paper for contraction in SUI women is 81.8 ± 31.9% lower than that measured in Dietz *et al.*' s paper, and similarly the strain value of 5.1±0.6% for Valsalva is 77.53 ± 229.6% lower. This difference seems very significant for contraction and although there is a big difference in Valsalva too, this difference is more disputable because of the large standard error. It can be concluded that the PFM might have more contraction in the circumferential direction, and further measurement combining these two directions can result in a better calculation of the strain of the PFM during contraction and Valsalva.

Comparing the strain measurements in this paper to other similar calculations carried out on different muscle tissues such as cardiac muscle which shows that the calculated peak systolic longitudinal strain of myocardial tissues using ultrasound speckle tracking, is -15.1±2.3% in normal subjects and -9±0.8% in the patients (Rappaport *et al.* 2006). These values are much larger than all the strain values calculated in this paper since the highest negative strain measured of the PFM was during a supine cough in healthy individuals with a value of -8.8 ± 0.7%. This value is much lower than the peak strain in normal myocardial muscles (41.4 ± 15.9% lower). Another similar strain measurement has been carried out using strain rate imaging for gastric wall during gastric contraction. The values obtained during this study were circumferential stains of -33 ± 23% and 25 ± 6 % for inferior and superior parts of the gastric wall respectively (Gilja *et al.* 2002). The values obtained for this study is even much higher than the stain of the PFM measured in this paper.

Previous strain measurements of the pubovisceral muscle were calculated using 3-D ultrasound imagaing. While 3-D imaging does provide a more accurate anatomical image analysis than 2-D ultrasound imaging, current 3-D imaging and MRI techniques however, are not fast enough to record ARA movement in fast maneuvers like coughing. Future studies combining the measurements in this study from the 2-D ultrasound data and other strain measurements of the PFM in different directions can further characterize the PFM function. Therefore, it was the aim of this study to use the 2-D ultrasound data to calculate important biomechanical properties of the PFM in order to better understand incontinence and provide clinically useful information for treatment of women with SUI and other pelvic floor dysfunctions.

In conclusion, the measurements in this paper showed that the negative strain of the PFM is significantly higher in continent women than that in SUI patients, especially during fast reflex events such as a cough, and thus validating the importance of the PFM in continence mechanism. Additionally, the results have demonstrated that the PFM stretches more in SUI patients than that in continent women since the positive strain was always higher in SUI women.

ACKNOWLEDGEMENTS

This study was supported in part by an NIH research grant NIBIB 1 R21 EB001654. Author wishes to acknowledge the contributions of Q. Peng R. Jones and S. Rachmanian.

REFERENCES

[1] Abitbol, M. M. (1988), "Evolution of the ischial spine and of the pelvic floor in the Hominoidea." *Am J. Phys Anthropology* 75(1): 53-67.

[2] Athanasiou, S., V. Khullar, *et al.* (1999). "Imaging the urethral sphincter with three-dimensional ultrasound." *Obstet Gynecol* 94(2): 295-301.

[3] Barbic, M., B. Kralj, *et al.* (2003). "Compliance of the bladder neck supporting structures: importance of activity pattern of levator ani muscle and content of elastic fibers of endopelvic fascia." *Neurourol Urodyn* 22(4): 269-76.

[4] Berghmans, L. C., H. J. Hendriks, *et al.* (1998). "Conservative treatment of stress urinary incontinence in women: a systematic review of randomized clinical trials." *Br J. Urol* 82(2): 181-91.

[5] Bo, K., F. Lilleas, *et al.* (2001). "Dynamic MRI of the pelvic floor muscles in an upright sitting position." *Neurourol Urodyn* 20(2): 167-74.

[6] Bo, K. and M. Sherburn (2005). "Evaluation of female pelvic-floor muscle function and strength." *Phys Ther* 85(3): 269-82.

[7] Buchsbaum, G. M., E. E. Duecy, *et al.* (2005). "Urinary incontinence in nulliparous women and their parous sisters." *Obstet Gynecol* 106(6): 1253-8.

[8] Bump, R. C., W. G. Hurt, *et al.* (1991). "Assessment of Kegel pelvic muscle exercise performance after brief verbal

instruction." *Am J Obstet Gynecol* 165(2): 322-7; discussion 327-9.

[9] Christensen, L. L., J. C. Djurhuus, *et al*. (1995). "Imaging of pelvic floor contractions using MRI." *Neurourol Urodyn* 14(3): 209-16.

[10] Comiter, C.V., S.P. Vasavada, *et al*. (1999). "Grading pelvic prolapse and pelvic floor relaxation using dynamic magnetic resonance imaging." *Urology* 54(3): 454-7.

[11] Constantinou, C.E. and D.E. Govan (1982). "Spatial distribution and timing of transmitted and reflexly generated urethral pressures in healthy women." *J Urol* 127(5): 964-9.

[12] Constantinou, C. E., G. Hvistendahl, *et al*. (2002). "Determining the displacement of the pelvic floor and pelvic organs during voluntary contractions using magnetic resonance imaging in younger and older women." *BJU Int* 90(4): 408-14.

[13] Costantini, S., F. Esposito, *et al*. (2006). "Ultrasound imaging of the female perineum: the effect of vaginal delivery on pelvic floor dynamics." *Ultrasound Obstet Gynecol* 27(2): 183-7.

[14] Deindl, F. M., D. B. Vodusek, *et al*. (1993). "Activity patterns of pubococcygeal muscles in nulliparous continent women." *Br J Urol* 72(1): 46-51.

[15] Deindl, F. M., D. B. Vodusek, *et al*. (1994). "Pelvic floor activity patterns: comparison of nulliparous continent and parous urinary stress incontinent women. A kinesiological EMG study." *Br J Urol* 73(4): 413-7.

[16] DeLancey, J. O. (2005). "The hidden epidemic of pelvic floor dysfunction: achievable goals for improved prevention and treatment." *Am J Obstet Gynecol* 192(5): 1488-95.

[17] DeLancey, J. O., K. Strohbehn, *et al*. (1998). "Comparison of ureteral and cervical descents during vaginal hysterectomy for uterine prolapse." *Am J Obstet Gynecol* 179(6 Pt 1): 1405-8; discussion 1409-10.

[18] Dietz, H. P. (2004). "Ultrasound imaging of the pelvic floor. Part II: three-dimensional or volume imaging." *Ultrasound Obstet Gynecol* 23(6): 615-25.

[19] Dietz, H. P., S. K. Jarvis, *et al*. (2002). "The assessment of levator muscle strength: a validation of three ultrasound techniques." *Int Urogynecol J Pelvic Floor Dysfunct* 13(3): 156-9; discussion 159.

[20] Dietz H, Thyer I, Shek C. Clinical validation of a new imaging method for assessing pelvic floor biomechanics. *Ultrasound in Obstetrics and Gynecology* 2006; (In Press).

[21] Ferreira, P. H., M. L. Ferreira, *et al*. (2004). "Changes in recruitment of the abdominal muscles in people with low back pain: ultrasound measurement of muscle activity." *Spine* 29 (22): 2560-6.

[22] Fielding, J. R., H. Dumanli, *et al*. (2000). "MR-based three-dimensional modeling of the normal pelvic floor in women: quantification of muscle mass." *AJR Am J Roentgenol* 174(3): 657-60.

[23] Goh, V., S. Halligan, *et al*. (2000). "Dynamic MR imaging of the pelvic floor in asymptomatic subjects." *AJR Am J Roentgenol* 174(3): 661-6.

[24] Gilja OH, Heimdal A, Hausken T, Gregersen H, Matre K, Berstad A, Odegaard S. Strain during gastric contractions can be measured using Doppler ultrasonography. *Ultrasound Med Biol*. 2002, 28(11-12): 1457-65.

[25] Gousse, A. E., Z. L. Barbaric, *et al*. (2000). "Dynamic half Fourier acquisition, single shot turbo spin-echo magnetic resonance imaging for evaluating the female pelvis." *J Urol* 164(5): 1606-13.

[26] Hodges, P. W. and C. A. Richardson (1999). "Altered trunk muscle recruitment in people with low back pain with upper limb movement at different speeds." *Arch Phys Med Rehabil* 80(9): 1005-12.

[27] Jones R. C., Peng Q., Shishido K., Perkash I., Constantinou CE 2D Ultrasound Imaging and Motion Tracking of Pelvic Floor Muscle (PFM) Activity During Abdominal Manoeuvres in Stress Urinary Incontinent Women *Neurourolgy & Urodynamics*, 25(6) 596-597, 2006.

[28] Jones R.C., Peng Q., Shishido K. and Constantinou C.E. (2006). 2D Ultrasound Evaluation of Dynamic Responses of Female Pelvic Floor Muscles (PFM) to a Cough. *Neurourolgy & Urodynamics*, 25(6) 624-625, 2006.

[29] Kessler, R. and C. E. Constantinou (1986). "Internal urethrotomy in girls and its impact on the urethral intrinsic and extrinsic continence mechanisms." *J Urol* 136(6): 1248-53.

[30] Klutke, C., J. Golomb, *et al*. (1990). "The anatomy of stress incontinence: magnetic resonance imaging of the female bladder neck and urethra." *J Urol* 143(3): 563-6.

[31] Laycock, J., J. Brown, *et al*. (2001). "Pelvic floor reeducation for stress incontinence: comparing three methods." *Br J Community Nurs* 6(5): 230-7.

[32] Mclean L, Madill SJ. A contextual model of pelvic floor muscle defects in female stress urinary in-continence: a rationale for physiotherapy management. *Ann N Y Acad Sci*. 2007.

[33] Miller, J. M., J. A. Ashton-Miller, *et al*. (1998). "A pelvic muscle precontraction can reduce cough-related urine loss in selected women with mild SUI." *J Am Geriatr Soc* 46(7): 870-4.

[34] Miller, J. M., D. Perucchini, *et al*. (2001). "Pelvic floor muscle contraction during a cough and decreased vesical neck mobility." *Obstet Gynecol* 97(2): 255-60.

[35] Morin, M., D. Bourbonnais, *et al*. (2004). "Pelvic floor muscle function in continent and stress urinary incontinent women using dynamometric measurements." *Neurourol Urodyn* 23(7): 668-74.

[36] Neumann, P. and V. Gill (2002). "Pelvic floor and abdominal muscle interaction: EMG activity and intra-abdominal pressure." *Int Urogynecol J Pelvic Floor Dysfunct* 13(2): 125-32.

[37] Norton, C., S. Chelvanayagam, *et al*. (2003). "Randomized controlled trial of biofeedback for fecal incontinence." *Gastroenterology* 125(5): 1320-9.

[38] Nygaard, I. (2004). Physiologic outcome measures for urinary incontinence. *Gastroenterology* 126(1 Suppl 1): S99-105.

[39] Peng Q., Jones R.C., Constantinou C.E. (2006A) 2D Ultrasound image processing in identifying responses of urogenital structures to pelvic floor muscle activity. *Ann Biomed Eng.*; 34(3): 477-493.

[40] Peng, Q., R. Jones, C. E. Constantinou (2007). Ultrasound evaluation of dynamic responses of female pelvic floor muscles. *Ultrasound in Med Biol*. 33(3):342-52.

[41] Petros P.E., VonKonsky B. Anchoring the mid urethra restores bladder neck anatomy and continence Lancet 354 9193:997-998 1999

[42] Reddy, A. P., J. O. DeLancey, *et al*. (2001). "On-screen vector-based ultrasound assessment of vesical neck movement." *Am J Obstet Gynecol* 185(1): 65-70.

[43] Rappaport D., Adam D., Lysyansky P., Riesner S. Assessment of myocardial regional strain and strain rate by tissue tracking in B-mode echocardiograms. *Ultrasound Med Biol*. 2006 Aug; 32(8): 1181-9.

[44] Sapsford, R. R., P. W. Hodges, *et al*. (2001). "Co-activation of the abdominal and pelvic floor muscles during voluntary exercises." *Neurourol Urodyn* 20(1): 31-42.

[45] Schaer, G. N., D. Perucchini, *et al*. (1999). "Sonographic evaluation of the bladder neck in continent and stress-incontinent women." *Obstet Gynecol* 93(3): 412-6.

[46] Shishido K., Jones R.C., Peng Q. and Constantinou C.E. (2006). Passive response of the pelvic floor to the increase of the intra-abdominal pressure during a Valsalva. *Neurourolgy & Urodynamics*, 25(6) 529-530 2006.

[47] Smith, M. D., A. Russell, *et al*. (2006). "Disorders of breathing and continence have a stronger association with back pain than obesity and physical activity." *Aust J Physiother* 52(1): 11-6.

[48] Stoker, J., S. Halligan, *et al*. (2001). "Pelvic floor imaging." *Radiology* 218(3): 621-41.

[49] Theofrastous, J. P., J. F. Wyman, *et al*. (2002). "Effects of pelvic floor muscle training on strength and predictors of response in the treatment of urinary incontinence." *Neurourol Urodyn* 21(5): 486-90.

[50] Yang, A., J. L. Mostwin, *et al*. (1991). "Pelvic floor descent in women: dynamic evaluation with fast MR imaging and cinematic display." *Radiology* 179(1): 25-33.